Protein Engineering, Design & Selection vol. 22 no. 12 pp. 747–752, 2009
Published online October 22, 2009 doi:10.1093/protein/gzp061

Substrate specificity of microbial transglutaminase as revealed by three-dimensional docking simulation and mutagenesis

Uno Tagami[1], Nobuhisa Shimba[1,3], Mina Nakamura[1], Kei-ichi Yokoyama[1], Ei-ichiro Suzuki[1] and Takatsugu Hirokawa[2,3]

[1]Institute of Life Sciences, Ajinomoto Co., Inc, 1-1 Suzuki-cho, Kawasaki-ku, Kawasaki-shi 210-8681, Japan and [2]Computational Biology Research Center (CBRC), National Institute of Advanced Industrial Science and Technology (AIST), 2-43-17F Aomi, Koutou-ku, Tokyo 135-0064, Japan

[3]To whom correspondence should be addressed.
E-mail: nobuhisa_shimba@ajinomoto.com (N.S.); E-mail: t-hirokawa@aist.go.jp (T.H.)

Transglutaminases (TGases) are used in fields such as food and pharmaceuticals. Unlike other TGases, microbial transglutaminase (MTG) activity is Ca^{2+}-independent, broadening its application. Here, a three-dimensional docking model of MTG binding to a peptide substrate, CBZ-Gln-Gly, was simulated. The data reveal CBZ-Gln-Gly to be stretched along the MTG active site cleft with hydrophobic and/or aromatic residues interacting directly with the substrate. Moreover, an oxyanion binding site for TGase activity may be constructed from the amide groups of Cys64 and/or Val65. Alanine mutagenesis verified the simulated binding region and indicated that large molecules can be widely recognized on the MTG cleft.

Keywords: molecular dynamics/site-directed mutagenesis/substrate docking/substrate specificity/transglutaminase

Introduction

Transglutaminases (TGase: protein-glutaminase γ-glutamyltransferase, EC 2.3.2.13) constitute a family of enzymes that catalyze the replacement of the amide ammonia at the γ-position in glutamine residues with another amine, usually an ε-amino group from a suitable lysine residue (Lorand *et al*., 1962; Folk, 1970, 1980; Dadabay *et al*., 1989). The formation of ε-(γ-glutamyl)lysine isopeptide bonds results in both intra- and intermolecular cross-linking of proteins, leading to polymerization. The incorporation of such covalent cross-links with microbial transglutaminase (MTG) into food proteins, such as tofu, boiled fish paste and sausage, improves their physical and textural properties (Ikura *et al*., 1980; Motoki and Nio, 1983; Kurth and Rogers, 1984). Recently, the covalent binding of poly(ethyleneglycol) by TGase was reported as a promising method for surface modification to make protein drugs more water soluble, non-aggregating, non-immunogenic and more stable against proteolytic digestion (Fontana *et al*., 2008). This unique application is possible due to the availability of glutamine residues for attack by TGase in globular proteins possessing regions characterized by enhanced chain flexibility, which are also favorable targets for proteases.

TGases are widely distributed in various organisms, including vertebrates (Chung and Folk, 1972; Wong *et al*., 1990; Weraarchakul-Boonmark *et al*., 1992; Grant *et al*., 1994; Yasueda *et al*., 1995), invertebrates (Tokunaga *et al*., 1993; Signh and Metha, 1994), mollusks (Klein *et al*., 1992), plants (Margosiak *et al*., 1990) and microorganisms (Kanaji *et al*., 1993). For example, human blood coagulation factor XIII, which forms fibrin clots in hemostasis and wound healing by catalyzing the cross-linking between fibrin molecules, has been well characterized (Bruner-Lorand *et al*., 1966; Gladner and Nossal, 1983; Ichinose *et al*., 1986; Hornyak *et al*., 1989; Bishop *et al*., 1990; Hornyak and Shafer, 1991), and its crystal structure has been determined (Pedersen *et al*., 1994; Yee *et al*., 1994, 1995; Weiss *et al*., 1998). The red sea bream liver transglutaminase (fish-derived TGase, FTG) is a member of the tissue-type TGase family. Reports indicate that the overall structure of FTG and human factor XIII is similar (Noguchi *et al*., 2001). In contrast to many other TGases, MTG activity is Ca^{2+}-independent. Moreover, its structure is very different from the others as MTG adopts a disk-like shape with a deep cleft at the edge of the disk. The residue essential for the catalytic activity, Cys64, exists at the bottom of the cleft (Kashiwagi *et al*., 2002).

A database for TGase substrate proteins, called TRANSDAB (http://genomics.dote.hu/wiki/index.php/Main_Page), has produced useful information regarding sequence preference as this database provides a list of previously identified substrates (Facchiano *et al*., 2003). Additional sequences preferred by MTG were discovered by analysis of reactive glutamine residues within substrates using phage display (Sugimura *et al*., 2008). However, in spite of these studies on the structural properties and substrate specificity, little is known about substrate recognition by TGases. One primary obstacle is the fact that the substrate specificity is regulated by the protein primary sequence and tertiary structure surrounding the glutamine residues, of which there may be several that could potentially act as a substrate.

Ligand-docking experiments are a powerful approach for investigating the binding mode. This is despite the experimental challenges that arise in determining the complex structure of an enzyme and its substrate due to weak interactions and substrate turnover. In fact, a computational conformational analysis and docking study of potent factor XIII inhibitors having a cyclopropenone ring have been implemented previously (Iwata *et al*., 2000). Here, we describe results from a docking study of MTG and a peptide substrate, CBZ-Gln-Gly, including molecular dynamic simulation and a proposed substrate recognition mechanism for

the enzyme. Alanine mutagenesis studies were also conducted to verify the substrate binding region. Knowledge of MTG binding with substrate will help further expand the applications for MTG use.

Materials and methods

Docking study

The X-ray structure of MTG (Protein Data Bank entry 1IU4) was used as an initial structure for the docking study. A three-dimensional structure of the substrate, CBZ-Gln-Gly, was constructed and minimized by Discovery Studio (Accelrys Software Inc.). First, the structure of MTG was prepared by removing all solvents and adding hydrogen atoms. Then, the position of Cys64 S^{γ} was changed, such that its location was close enough for hydrogen bond formation with Asp255 $H^{\sigma 2}$ as these residues are assumed to be a catalytic diad (Kashiwagi *et al*., 2002). As a result, the $\chi 1$ angle of the cysteine residue was rotated 68° from the X-ray structure. His274 was also isomerized to make a wider pocket for CBZ-Gln-Gly binding. After setting the charge states of the Sγ atom of Cys64 and Asp255 to be negative and neutral (COOH), respectively, as shown previously (Kashiwagi *et al*., 2002), they were minimized by a protein preparation method using Prime (Schrödinger, LLC) for the docking study. The docking study and score calculations were performed using Maestro (Schrödinger, LLC). A grid box for the molecular docking by Glide (Schrödinger, LLC) was set as a cube where each side was 17 Å, which was the length of the stretched form of CBZ-Gln-Gly. The grid box was defined by the center of the two active site residues, Cys64 and Asp255. CBZ-Gln-Gly was docked in the standard precision mode by Glide, up to 100 structures. These docked structures were then classified into nine groups using MOE (Chemical Computing Group Inc.); the structures in each were within 4.5 Å of the RMS deviations.

Molecular dynamics

All MD simulations were performed using the AMBER8 software package with the parm96 force field. The complex structures were surrounded with a 15 Å layer of TIP3P water molecules (Jorgensen *et al*., 1983). The electrostatic charge was neutralized by adding counter ions using the LeaP module of AMBER8. After minimization, heating and equilibration, the production MD phase was carried out at 300 K for 10 ns with a time step of 1 fs using the constant volume and temperature (NVT) ensemble and the PME algorithm. All simulations were performed on an 8192 CPU core (4096 computing nodes) IBM BlueGene/L supercomputer at the Computational Biology Research Center (CBRC).

Site-directed mutagenesis

Mutations encoding the amino acid substitutions, D3A, D4A, R5A, R26A, Y62A, G63A, C64A, V65A, W69A, Y75A, N239A, I240A, P241A, G250A, V252A, N253A, F254A, D255A, Y256A, H274A, N276A, H277A, Y278A, S284A, L285A, E300A, Y302A, D304A and F305A, were introduced into the *mtg* gene by using the QuikChange mutagenesis kit (Stratagene). The integrity of the *mtg* open reading frame and the presence of the mutations were verified by DNA sequencing. MTG and its variants were expressed and purified as described previously (Yokoyama *et al*., 2000, 2002).

TGase activity assay

TGase activity was measured by the calorimetric hydroxamate procedure and an NMR-based screening method using *N*-carbobenzoxy-L-glutaminyl-glycine and ovalbumin (chicken egg albumin) as described previously (Folk and Cole, 1966; Shimba *et al*., 2002a, 2002b).

Results and discussion

Binding simulation of CBZ-Gln-Gly to MTG

The docking program Glide was used initially to predict the three-dimensional structure of MTG bound to CBZ-Gln-Gly. A total of 100 docking structures were calculated and then classified into nine groups based on the RMS deviations of the ligand conformation (Fig. 1A and B). In Groups 1, 2, 3, 4 and 6, the distances between the Cys64 S^{γ} atom in MTG and the Gln C^{δ} atom in CBZ-Gln-Gly were ~4 Å, indicating that they were capable of an enzymatic reaction, since Cys64 S^{γ} was assumed to be a nucleophilic atom. However, the locations of Cys64 S^{γ} in MTG and Gln C^{δ} in CBZ-Gln-Gly of the structures in Groups 5, 7, 8 and 9 were too far to be active for the enzyme. Therefore, the docking structures in Groups 1, 2, 3, 4 and 6 were selected as the first candidates for further investigation.

MD simulation of the complex

In Groups 1, 2, 3, 4 and 6, Cys64 S^{γ} in MTG and Gln C^{δ} in CBZ-Gln-Gly were observed to be in the proper position for the enzymatic reaction. However, an oxyanion binding site was not found in any of the docking structures. To select a proper model structure, MD simulation was performed on the structures in Groups 1, 2, 3, 4 and 6. A centroid structure for each group was calculated to be the initial conformation by MOE. Figure 1C shows the distance profiles between Cys64 S^{γ} in MTG and Gln C^{δ} in CBZ-Gln-Gly during the 10 ns MD simulation. Snapshots were taken every picosecond during the 10 ns production phase for a total of 10 000 snapshots. Cys64 S^{γ} in MTG and Gln C^{δ} in CBZ-Gln-Gly in the docking structures of Group 3 remained in their proper positions for more than 8 ns, whereas the substrate was released quickly in structures from Groups 1, 2, 4 and 6. Consistency of the results were obtained in another independent simulations with different initial velocities assigned to the same starting structure for each docking group (data not shown). We have also calculated the average binding free energy from MD trajectories by MM-GBSA calculation in AMBER program. The average binding free energy of Groups 1, 2, 3, 4 and 6 were −5.42, −9.25, −16.48, −11.68 and −5.30 kcal/mol, respectively. Therefore, the docking structures of Group 3 during the MD simulation were selected as representing the proper structure.

Next, all trajectories were analyzed to find the oxyanion binding site. The γ-carboxyl group of CBZ-Gln-Gly is located within 4 Å from both amide groups of Cys64 and Val65 in the 692 trajectories of Group 3. However, oxyanion binding sites were not observed in any trajectories calculated from the initial structures from Groups 1, 2, 4 and 6. In addition, a hydrogen bond between Cys64 S^{γ} and Asp255

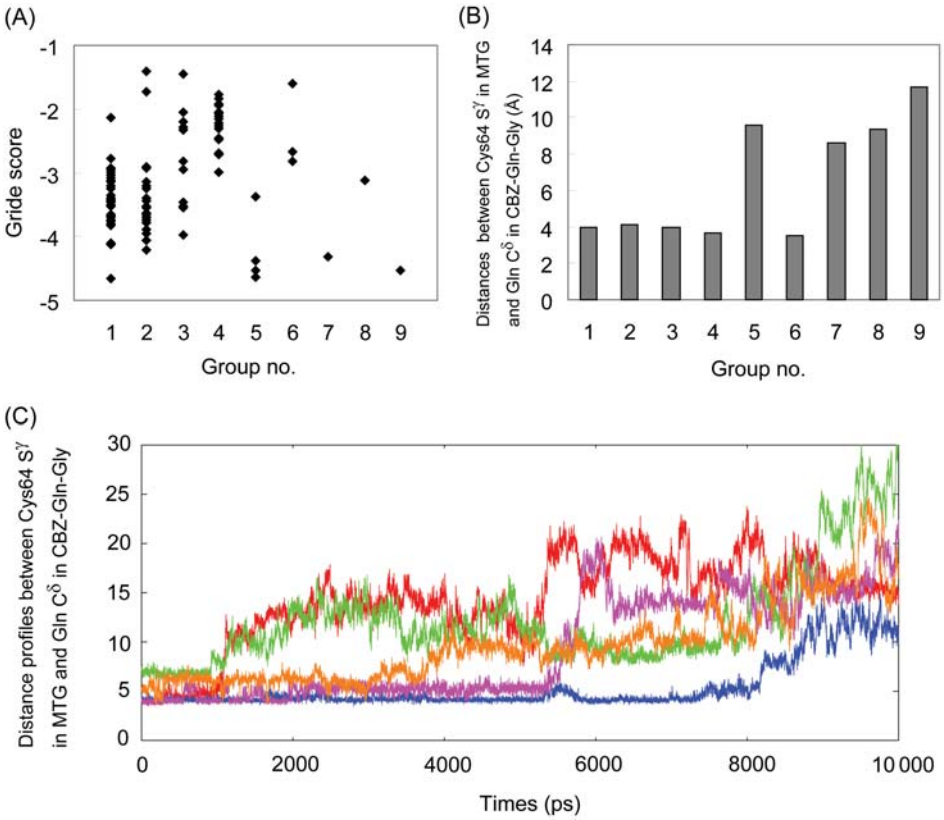

Fig. 1. (**A**) A total of 100 docking structures of MTG binding with CBZ-Gln-Gly were classified into nine groups based on the RMS deviations of the ligand conformation. Glide scores are plotted in each group. (**B**) The distances between the Cys64 S^{γ} atom in MTG and the Gln C^{δ} atom in CBZ-Gln-Gly in each group are shown. (**C**) Distance profiles between Cys64 S^{γ} in MTG and Gln C^{δ} in CBZ-Gln-Gly during the 10 ns MD calculation, which are plotted in red (Group 1), green (Group 2), blue (Group 3), pink (Group 4) and orange (Group 6), are depicted. Snapshots were taken every picosecond during the 10 ns production phase.

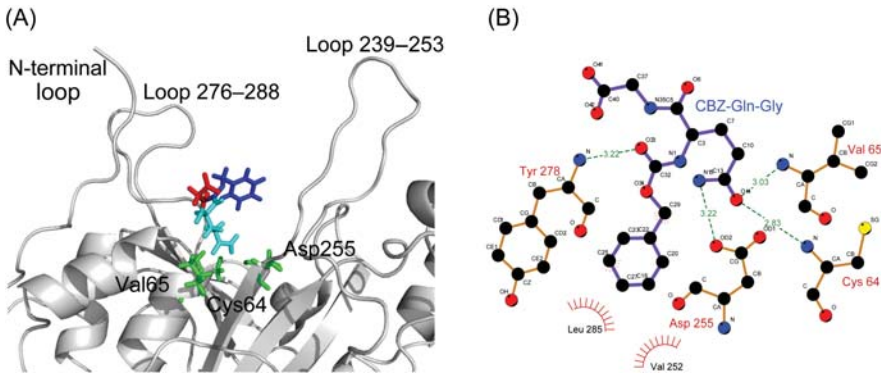

Fig. 2. (**A**) Docking structure of MTG binding with the substrate, CBZ-Gln-Gly. In CBZ-Gln-Gly, the CBZ, Gln and Gly moieties are shown in blue, cyan and red, respectively. In MTG, Cys64, Val65 and Asp255 are depicted in green. (**B**) Schematic view of the interactions between CBZ-Gln-Gly and MTG.

O^{δ}, which was assumed to form a catalytic diad with Cys64, was formed in 7 out of the 692 trajectories assessed. All seven conformations were oriented in the same direction on the MTG molecule. As such, the docking structure with the shortest distance between Cys64 S^{γ} in MTG and Gln C^{δ} in CBZ-Gln-Gly was selected from the seven trajectories (Fig. 2).

Alanine mutagenesis to verify the CBZ-Gln-Gly binding site

To identify the critical residues for substrate recognition, the residues surrounding Cys64, which is essential for MTG activity, were replaced with alanines, and the activities based on the calorimetric hydroxamate procedure were measured (Fig. 3, Table I). It should be noted that the substrate on the calorimetric hydroxamate procedure was a small peptide-like molecule, CBZ-Gln-Gly. These studies demonstrated no activity for G63A, C64A, N253A, F254A, D255A, Y256A and H277A, in which Cys64 was the catalytic residue and Asp255 was assumed to be an electron donor. In addition, TGase activities of the variants, Y62A, V65A, V252A, N276A and Y278A, were reduced dramatically, indicating that these residues are important for substrate recognition.

Residues contacting the substrate in the docking model mostly overlapped with those within the substrate recognition

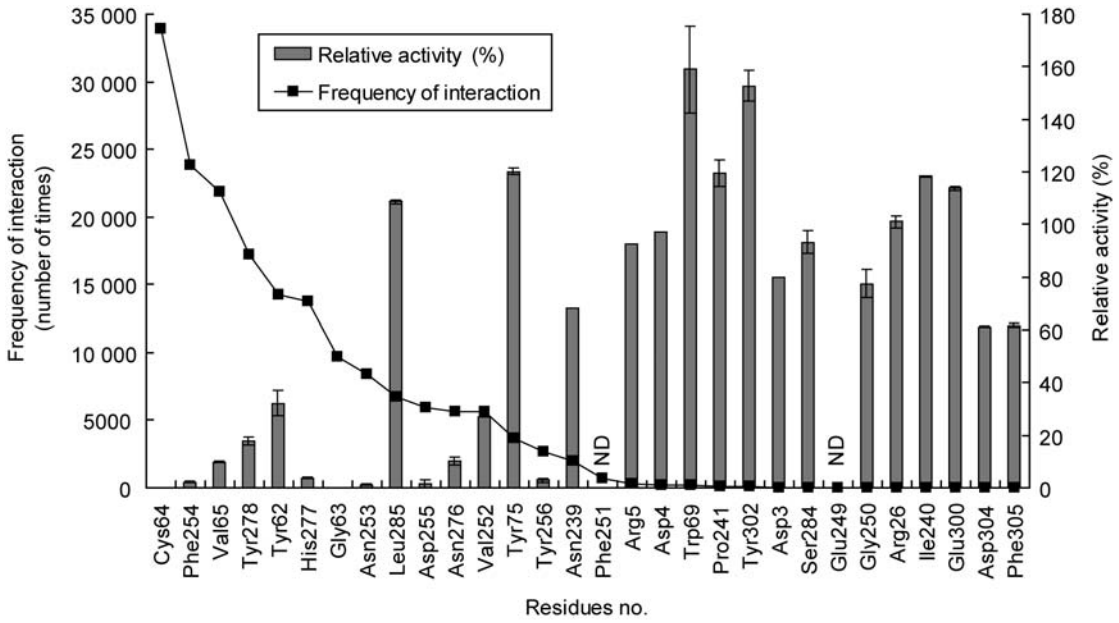

Fig. 3. Frequency of interaction between MTG and CBZ-Gln-Gly during the MD simulation (dots) and relative activities of MTG variants in which residues surrounded by Cys64 were replaced with alanine (bars). The activity of the variants was compared with the wild-type. Residue numbers are sorted in descending order of interaction frequency.

Table I. TGase activities for the wild-type and variants determined by the calorimetric hydroxamate procedure and the NMR-based screening method

Variants	Calorimetric hydroxamate procedure (U/mg)	Relative activity (%)	NMR-based screening method ($\times 10^{-3}$ U/mg)	Relative activity (%)
Wild-type	26.3 ± 0.2	100.0	44.8	100.0
D3A	25.5	97.0	ND	ND
D4A	21.0	80.0	ND	ND
R5A	24.4	92.6	ND	ND
R26A	26.6 ± 0.6	101.1	8.1	18.0
Y62A	8.5 ± 1.3	32.2	ND	ND
G63A	0.0	0.0	ND	ND
C64A	0.0	0.0	0.2	0.4
V65A	2.6 ± 0.0	9.8	4.6	10.2
W69A	41.8 ± 4.3	158.9	ND	ND
Y75A	31.6 ± 0.3	120.2	2.4	5.3
N239A	17.9	68.2	ND	ND
I240A	31.1 ± 0.1	118.3	30.6	68.3
P241A	31.4 ± 1.3	119.3	ND	ND
G250A	20.3 ± 1.4	77.4	ND	ND
V252A	7.1 ± 0.0	26.8	2.7	6.0
N253A	0.3 ± 0.1	1.1	0.5	1.1
F254A	0.5 ± 0.1	2.1	ND	ND
D255A	0.4 ± 0.4	1.6	0.1	0.2
Y256A	0.7 ± 0.2	2.8	0.8	1.9
H274A	15.6 ± 0.8	59.3	4.2	9.3
N276A	2.6 ± 0.4	9.9	0.8	1.7
H277A	1.0 ± 0.1	3.7	ND	ND
Y278A	4.6 ± 0.4	17.6	1.8	3.9
S284A	24.5 ± 1.2	93.3	ND	ND
L285A	28.6 ± 0.2	108.7	16.5	36.8
E300A	29.9 ± 0.2	113.7	24.5	54.7
Y302A	40.2 ± 1.5	152.7	ND	ND
D304A	16.1 ± 0.1	61.2	18.4	41.1
F305A	16.2 ± 0.2	61.6	8.4	18.6

Activities were assayed as described in the Materials and methods. RMS deviations were calculated on the basis of two or three experiments.

site, as indicated by the alanine mutagenesis studies. The frequency of interaction between MTG and CBZ-Gln-Gly during the MD simulation (10 ns) was calculated using LIGPLOT (Wallace *et al.*, 1995) (Fig. 3). The catalytic residue Cys64 displayed the greatest number of contacts in the simulation. The results were sorted in descending order of interaction frequency. Residues Tyr62, Gly63, Cys64, Val65, Val252, Asn253, Phe254, Asp255, Tyr256, Asn276, His277 and Tyr278, which interacted frequently with CBZ-Gln-Gly during the MD simulation, were found to be located within the region where alanine substitution led to dramatic reduction of TGase activity. In contrast, most of the residues which did not interact with CBZ-Gln-Gly also did not influence TGase activity following alanine substitution. Overall, these alanine mutagenesis studies were consistent with the docking model of MTG bound with CBZ-Gln-Gly.

The catalytic site in the docking model consists of Cys64 in addition to an oxyanion binding site constructed from the amide groups of Cys64 and/or Val65. Within this site, the Val65 amide group was maintained in the proper orientation by a hydrophobic interaction between the Val65 side chain and Tyr62, Val67, Trp69, Tyr75, Pro76 and Tyr256. CBZ-Gln-Gly was located in the cleft, which was constructed from loops formed by 239–253 and 276–288 within MTG, and surrounded by hydrophobic and aromatic residues such as Tyr62, Val65, Tyr75, Val252, Phe254, Tyr256, Tyr278 and Leu285. These data suggest that substrate specificity was defined by hydrophobic and/or $\pi-\pi$ interactions, consistent with the peptide-sequence dependence of MTG reactivity (Ohtsuka *et al.*, 2000; Sugimura *et al.*, 2008) in which valine, leucine, isoleucine, phenylalanine, tyrosine or tryptophan in close proximity to a glutamine residue are preferable for substrate recognition.

In the model structure of the complex, CBZ-Gln-Gly was stretched across the active site cleft of MTG. In particular,

the benzyloxycarbonyl group of CBZ-Gln-Gly was located in the rear vestibule of the cleft, whereas the glycine residue was opposite in the front view of MTG, where the left side wall of the cleft consists of an N-terminal loop (Asp1–Ala10) and the loop 276–288, and the right side wall consists of the loop 239–253. In addition, it has been speculated that the flexibility of the right side wall of the cleft might decrease the steric hindrance between the enzyme and its substrates due to the high B-factors from Arg242 to Gly250 in the crystal structure of MTG (Kashiwagi *et al*., 2002). Protein substrates which are much larger than CBZ-Gln-Gly may also be recognized by the outside of the active cleft, which is aligned along CBZ-Gln-Gly in Figs 2A and 4A.

Substrate recognition of a larger molecule

To further investigate substrate recognition by MTG, TGase reactivity to a protein substrate was estimated by NMR (Table I). Instead of the CBZ-Gln-Gly substrate used in the alanine mutagenesis study, ovalbumin was used in these experiments (Shimba *et al*., 2002a, 2002b). ^{15}N nuclei were incorporated into the γ-carboxyamide groups of the glutamine residues in arbitrary proteins by the TGase reaction, followed by NMR detection to evaluate the reactivity of the enzymes on the protein substrate. In addition to the residues found to be crucial for CBZ-Gln-Gly recognition, TGase activities of the variants, Arg26, Tyr75, His274, Leu285, Asp304 and Phe305, for the protein substrate were reduced to less than half that of the wild-type. These residues were located along the active site cleft (Fig. 4B), indicating that the recognition site of a large molecule such as a protein substrate is expansive on the surface of the cleft in MTG.

In the present study, we have shown that peptide/protein substrates are recognized along the active site cleft of MTG, and that the amide groups of Cys64 and/or Val65 are candidates for the oxyanion binding site for TGase reactions. In the model structure of the complex, numerous hydrophobic and aromatic residues interacted directly with the substrate, implicating analogous recognition mechanisms by many proteases. A method to identify the specificity of proteases has been reported previously, and the P2 position typically shows a preference for hydrophobic amino acids (Harris *et al*., 2000). For example, the P2 position of papain prefers Val>Phe>Tyr>Nle and cruzein prefers Leu>Tyr>Phe>Val. It may be possible that MTG and the proteases have similar substrate preferences for hydrophobic amino acids in the peptide/protein sequence. In addition, glutamine residues

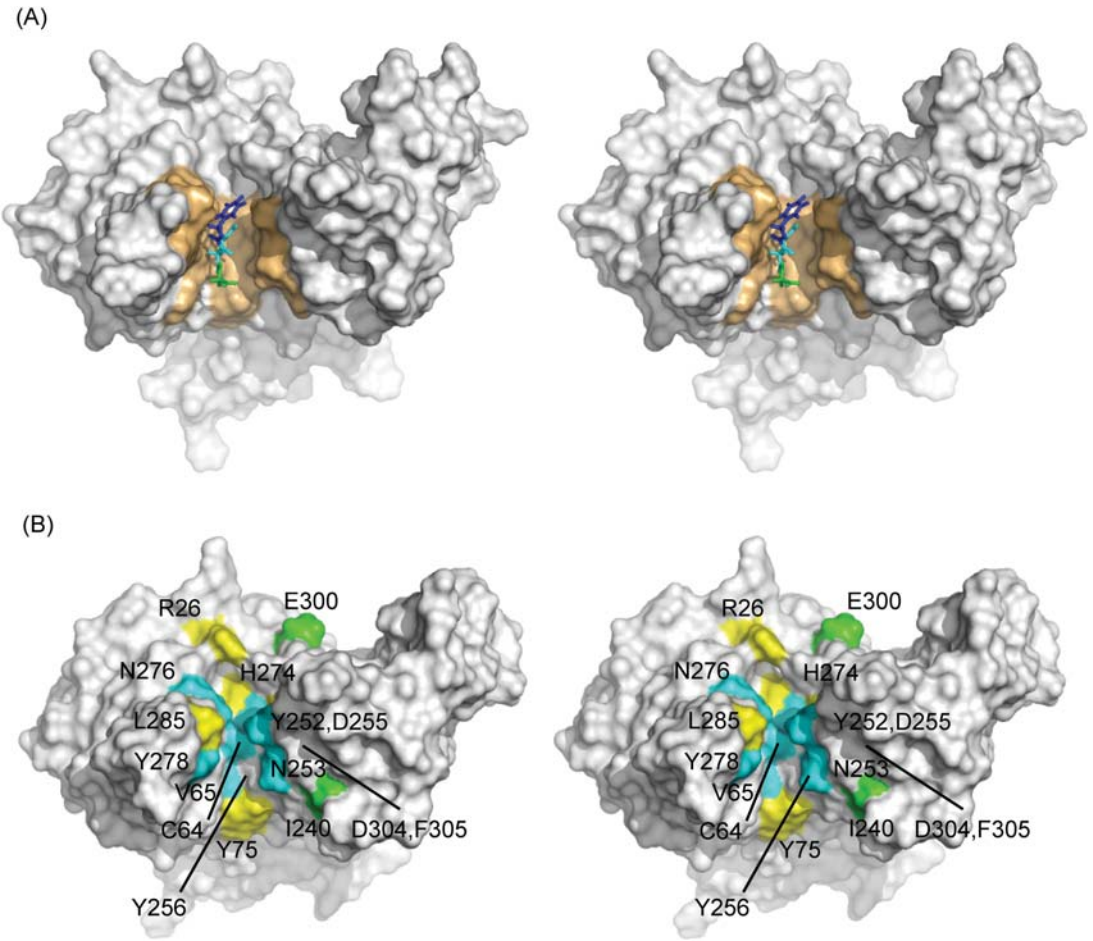

Fig. 4. (**A**) Docking structure of MTG binding with CBZ-Gln-Gly, in which the CBZ Gln, and Gly moieties are shown in blue, cyan, and green, respectively. Residues contacting CBZ-Gln-Gly are shown in orange. (**B**) Mapping of the residues onto the crystal structure, which was crucial for the TGase activity demonstrated in the alanine mutagenesis study. TGase activity of the variants, C64A, V65A, V252A, N253A, D255A, Y256A, N276A and Y278A, was less than half that of the wild-type for both substrates CBZ-Gln-Gly and ovalbumin (shown in cyan). In contrast, those of R26A, Y75A, H274A, L285A, D304A and F305A were less than half only for ovalbumin (shown in yellow), and the activity of I240A and E300A was retained regardless of substrate (shown in green).

attacked by MTG are located in regions characterized by enhanced chain flexibility, which are also favorable targets for proteases. MTG, as well as the other TGases (Fontana *et al*., 2008), has potential for use in surface modification applications to make proteins more stable against proteolytic digestion.

Acknowledgements

We thank Dr Tatsuki Kashiwagi for useful discussion.

Funding

Funding to pay the Open Access publication charges for this article was provided by Ajinomoto Co., Inc.

References

Bishop,P.D., Teller,D.C., Smith,R.A., Lasser,G.W., Gilbert,T. and Seale,R.L. (1990) *Biochemistry*, **29**, 1861–1869.
Bruner-Lorand,J., Pilkington,T.R.E. and Lorand,L. (1966) *Nature*, **210**, 1273–1274.
Chung,S.I. and Folk,J.E. (1972) *Proc. Natl Acad. Sci. USA*, **69**, 303–307.
Dadabay,C.Y. and Pike,L. (1989) *Biochem. J.*, **264**, 679–685.
Facchiano,A.M., Facchiano,A. and Facchiano,F. (2003) *Nucleic Acids Res.*, **31**, 379–382.
Folk,J.E. (1970) *Methods Enzymol.*, **17**, 889–894.
Folk,J.E. (1980) *Annu. Rev. Biochem.*, **49**, 517–531.
Folk,J.E. and Cole,P.W. (1966) *J. Biol. Chem.*, **241**, 5518–5525.
Fontana,A., Spolaore,B., Mero,A. and Veronese,F.M. (2008) *Adv. Drug Deliv. Rev.*, **60**, 13–28.
Gladner,J.A. and Nossal,R. (1983) *Thromb. Res.*, **30**, 273–288.
Grant,F.J., Taylor,D.A., Sheppard,P.O., Mathewes,S.L., Lint,W., Vanaja,E., Bishop,P.D. and O'hara,P.J. (1994) *Biochem. Biophys. Res. Commun.*, **203**, 1117–1123.
Harris,J.L., Backes,B.J., Leonetti,F., Mahrus,S., Wllman,J.A. and Craik,C.S. (2000) *Proc. Natl Acad. Sci. USA*, **97**, 7754–7759.
Hornyak,T.J. and Shafer,J.A. (1991) *Biochemistry*, **30**, 6175–6182.
Hornyak,T.J., Bishop,P.D. and Shafer,J.A. (1989) *Biochemistry*, **28**, 7326–7332.
Ichinose,A., Hendrickson,L.E., Fujikawa,K. and Davie,E.W. (1986) *Biochemistry*, **25**, 6900–6906.
Ikura,K., Kometani,T., Yoshikawa,M., Sasaki,R. and Chiba,H. (1980) *Agric. Biol. Chem.*, **44**, 1567–1573.
Iwata,Y., Tago,K., Kiho,T., Kogen,H., Fujioka,T., Otsuka,N., Suzuki-Konagai,K., Ogita,T. and Miyamoto,S. (2000) *J. Mol. Graph. Model.*, **18**, 591–599.
Jorgensen,W.L., Chandrasekhar,J., Madura,J.D., Impey,R.W. and Klein,M.L. (1983) *J. Chem. Phys.*, **79**, 926–935.
Kanaji,T., Ozaki,H., Takao,T., Kawajiri,K., Ide,H., Motoki,M. and Shimonishi,Y. (1993) *J. Biol. Chem.*, **268**, 11565–11572.
Kashiwagi,T., Yokoyama,K., Ishikawa,K., Ono,K., Ejima,D., Matsui,H. and Suzuki,E. (2002) *J. Biol. Chem.*, **277**, 44252–44260.
Klein,J.D., Guzman,E. and Kuehn,G.D. (1992) *J. Bacteriol.*, **174**, 2599–2605.
Kurth,L. and Rogers,P.J. (1984) *J. Food Sci.*, **49**, 573–576.
Lorand,L., Konishi,K. and Jacobsen,A. (1962) *Nature*, **194**, 1148–1149.
Margosiak,S.A., Dharma,A., Bruce-Carver,M.R., Gonzales,A.P., Louie,D. and Kuehn,G.D. (1990) *Plant Physiol.*, **92**, 88–96.
Motoki,M. and Nio,N. (1983) *J. Food Sci.*, **48**, 561–566.
Noguchi,K., Ishikawa,K., Yokoyama,K., Ohtsuka,T., Nio,N. and Suzuki,E. (2001) *J. Biol. Chem.*, **276**, 12055–12059.
Ohtsuka,T., Ota,M., Nio,N. and Motoki,M. (2000) *Biosci. Biotechnol. Biochem.*, **64**, 2608–2613.
Pedersen,L.C., Yee,V.C., Bishop,P.D., Le Trong,I., Teller,D.C. and Stenkamp,R.E. (1994) *Protein Sci.*, **3**, 1131–1135.
Shimba,N., Shinohara,M., Yokoyama,K., Kashiwagi,T., Ishikawa,K., Ejima,D. and Suzuki,E. (2002a) *FEBS Lett.*, **517**, 175–179.
Shimba,N., Yokoyama,K. and Suzuki,E. (2002b) *J. Agric. Food Chem.*, **50**, 1330–1334.
Signh,R.N. and Metha,K. (1994) *Eur. J. Biochem.*, **225**, 625–634.
Sugimura,Y., Yokoyama,K., Nio,N., Maki,M. and Hitomi,K. (2008) *Arch. Biochem. Biophys.*, **477**, 379–383.
Tokunaga,F., Muta,T., Iwanaga,S., Ichinose,A., Davie,E.W., Kuma,K. and Mikata,T. (1993) *J. Biol. Chem.*, **268**, 262–268.
Wallace,A.C., Laskowski,R.A. and Thornton,J.M. (1995) *Protein Eng.*, **8**, 127–134.
Weiss,M.S., Metzner,H.J. and Hilgenfeld,R. (1998) *FEBS Lett.*, **423**, 291–296.
Weraarchakul-Boonmark,N., Jeong,J.-M., Murthy,S.N.P., Engel,J.D. and Lorand,L. (1992) *Proc. Natl Acad. Sci. USA*, **89**, 9804–9808.
Wong,W.S., Batt,C. and Kinsella,J.E. (1990) *Int. J. Biochem.*, **22**, 53–59.
Yasueda,H., Nakanishi,K., Kumazawa,Y., Nagase,K., Motoki,M. and Matsui,H. (1995) *Eur. J. Biochem.*, **232**, 411–419.
Yee,V.C., Pedersen,L.C., Le Trong,I., Bishop,P.D., Stenkamp,R.E. and Teller,D.C. (1994) *Proc. Natl Acad. Sci. USA*, **91**, 7296–7300.
Yee,V.C., Pedersen,L.C., Bishop,P.D., Stenkamp,R.E. and Teller,D.C. (1995) *Thromb. Res*, **78**, 389–397.
Yokoyama,K., Nakamura,N., Seguro,K. and Kubota,K. (2000) *Biosci. Biotechnol. Biochem.*, **64**, 1263–1270.
Yokoyama,K., Ono,K., Ohtsuka,T., Nakamura,N., Seguro,K. and Ejima,D. (2002) *Protein Expr. Purif.*, **26**, 329–335.

Received June 30, 2009; revised August 30, 2009; accepted September 23, 2009

Edited by Haruki Nakamura